OPEN ACCESS Freely available online

PLoS one

A Survey of New Temperature-Sensitive, Embryonic-Lethal Mutations in *C. elegans*: 24 Alleles of Thirteen Genes

Sean M. O'Rourke, Clayton Carter[9], Luke Carter[9], Sara N. Christensen[9], Minh P. Jones[9], Bruce Nash[9], Meredith H. Price[9], Douglas W. Turnbull[9], Aleena R. Garner, Danielle R. Hamill, Valerie R. Osterberg, Rebecca Lyczak, Erin E. Madison, Michael H. Nguyen, Nathan A. Sandberg, Noushin Sedghi, John H. Willis, John Yochem, Eric A. Johnson, Bruce Bowerman*

The Institute of Molecular Biology, University of Oregon, Eugene, Oregon, United States of America

Abstract

To study essential maternal gene requirements in the early *C. elegans* embryo, we have screened for temperature-sensitive, embryonic lethal mutations in an effort to bypass essential zygotic requirements for such genes during larval and adult germline development. With conditional alleles, multiple essential requirements can be examined by shifting at different times from the permissive temperature of 15°C to the restrictive temperature of 26°C. Here we describe 24 conditional mutations that affect 13 different loci and report the identity of the gene mutations responsible for the conditional lethality in 22 of the mutants. All but four are mis-sense mutations, with two mutations affecting splice sites, another creating an in-frame deletion, and one creating a premature stop codon. Almost all of the mis-sense mutations affect residues conserved in orthologs, and thus may be useful for engineering conditional mutations in other organisms. We find that 62% of the mutants display additional phenotypes when shifted to the restrictive temperature as L1 larvae, in addition to causing embryonic lethality after L4 upshifts. Remarkably, we also found that 13 out of the 24 mutations appear to be fast-acting, making them particularly useful for careful dissection of multiple essential requirements. Our findings highlight the value of *C. elegans* for identifying useful temperature-sensitive mutations in essential genes, and provide new insights into the requirements for some of the affected loci.

Citation: O'Rourke SM, Carter C, Carter L, Christensen SN, Jones MP, et al. (2011) A Survey of New Temperature-Sensitive, Embryonic-Lethal Mutations in *C. elegans*: 24 Alleles of Thirteen Genes. PLoS ONE 6(3): e16644. doi:10.1371/journal.pone.0016644

Editor: Anne Hart, Brown University, United States of America

Received November 2, 2010; **Accepted** January 4, 2011; **Published** March 1, 2011

Funding: This work was supported by a Leukemia and Lymphoma Society of America fellowship to SOR, and NIH grants GM050817 and GM049869 to BB. The funders had no role in study design, data collection and analysis, decision to publish, or preparation of the manuscript.

Competing Interests: The authors have declared that no competing interests exist.

* E-mail: bbowerman@molbio.uoregon.edu

[9] These authors contributed equally to this work.

Introduction

To investigate essential gene requirements in model organisms, multiple approaches have been used to reduce gene function and infer gene requirements based on the resulting mutant phenotypes. Non-conditional mutations that inactivate genes can be used to study essential requirements, but such mutations must be maintained in heterozygotes and homozygous mutant progeny identified among progeny that vary in genotype. Furthermore, one gene can have multiple essential requirements during an organism life cycle, precluding investigation of all but the first essential requirement in progeny homozygous for a non-conditional mutation. To bypass early essential requirements in multicellular organisms, mitotic recombination [1,2], cell transplantation [3,4], or loss of extrachromosomal arrays [5] can be used to generate clones of homozygous mutant cells within otherwise heterozygous or wild-type individuals. But even within mutant clones of cells, only a single, early essential requirement can be examined, and the degree of control over the place and timing of mutant clone generation can vary substantially. Weak alleles of essential genes can sometimes bypass early essential requirements to permit the study of later requirements, and both RNA interference (RNAi) and small molecule inhibitors can in some cases be used to reduce gene function at multiple times during the life an organism [6,7]. However, the small molecule inhibitors suffer in some cases from a lack of gene specificity, a lack of penetrance in reducing gene function, or reduced bioavailability to the targeted protein. Thus, both small molecule inhibitors and RNAi remain limited in scope with respect to their use in many multicellular organisms. Finally, for genes that are expressed both maternally and zygotically, maternal expression of a wild-type allele can in some cases compensate for lack of zygotic expression in homozygous mutant progeny, precluding the identification of some gene requirements early in development when non-conditional alleles result in lethality due to later essential zygotic requirements.

When available, fast-acting temperature-sensitive (TS) gene mutations are perhaps the most powerful tool for dissecting multiple requirements for essential genes. While some conditional mutations are cold-sensitive (inactivating a gene product only at low temperatures), most conditional mutations are heat-sensitive (inactivating gene products only at high temperatures). TS mutations can also be either fast or slow acting, with fast-acting mutations causing amino acid changes that presumably destabilize a protein such that it unfolds or adopts a non-functional structure

shortly after up-shifting the organism to a restrictive temperature. Slow acting mutations presumably remain active at all temperatures when made at the permissive temperature, and must be replaced by newly synthesized, inactive protein after up-shifting to the restrictive temperature. Particularly with fast-acting TS mutations, one can identify multiple essential requirements, and define temperature-sensitive periods of gene requirements, sometimes even within a single cell cycle, or during the entire life span of an organism, by performing temperature up-shifts and down-shifts at different times [8,9]. Conditional mutations are also useful in that they allow for the easy propagation of homozygous mutant strains at the permissive temperature, and can be used to sensitize genetic backgrounds at intermediate temperatures for use in screens designed to identify second-site modifier loci as enhancers or suppressors of viability [10,11,12]. Moreover, site-directed mutagenesis can be used to engineer TS amino acid alterations in orthologous genes in other organisms. For example, a TS mutation in *C. elegans* dynein heavy chain, *dhc-1*, was engineered in the *S. cerevisiae* ortholog and was found to confer TS function [8]. In another case a ts allele of *src* was engineered in the *D. melanogaster* gene *sevenless* [10]. While TS mutations may not be useful for in vivo studies with mammalian model systems, some TS alleles have been identified in mammalian cell culture [13].

Not surprisingly, TS mutations isolated by mutagenizing populations of an organism are rare relative to non-conditional loss-of-function mutations. Many mutations can partially or fully inactivate a gene: for example, single nucleotide mutations can introduce early stop codons at one of many possible sites in most open reading frames. In contrast, relatively few mutations perturb protein function such that the outcome is conditional. For example, TS mutations often involve amino acid substitutions (mis-sense mutations) within the hydrophobic core of a folded protein that destabilize protein folding at higher temperatures [14].

Because TS mutations are relatively rare, they have been used most extensively in model organisms that are amenable to screens that enable one to search through large populations of mutagenized individuals for relatively rare conditional mutants. For example, TS mutants have been used extensively in budding yeast and fission yeast to identify essential gene functions [15,16], including many cell division cycle (CDC) genes that were discovered and characterized in both of these yeasts by screening for TS CDC mutant strains [17,18]. Shifting CDC mutant yeast to restrictive temperatures resulted in specific cell cycle arrest that elegantly revealed when the gene product was required [19]. TS mutants have also been utilized in *Drosophila melanogaster* [20], although far fewer examples exist and most have been identified fortuitously. Mammalian cell lines also have been used to isolate TS alleles of essential genes [13], but again relatively few examples exist.

TS mutations are now being used more and more extensively to probe gene function in the nematode *Caenorhabditis elegans*. Indeed, this organism is largely unique in being an animal model in which one can with relative ease identify rare conditional mutations in essential genes. Since the initial establishment of this nematode as a model organism, screening for conditional *C. elegans* mutants has been more feasible than in other animals, in part because it is self-fertile [21,22,23]. More recently, the innovation of using of egg-laying defective strains made *C. elegans* a powerful system for isolating non-conditional mutation in essential genes required for embryogenesis [24]. Modifications to the screening procedures that use egg-laying defective strains subsequently made it possible to isolate with relative ease thousands of conditional mutations in essential genes [25,26,27].

While one can efficiently isolate conditional, embryonic-lethal *C. elegans* mutants, positional cloning of the mutant loci has remained laborious and time consuming, substantially limiting the utility of mutant screens, particularly given how readily one can use RNA interference to probe essential *C. elegans* gene functions [6,28,29,30,31,32]. However, the advent of next generation DNA sequencing technology is now making it possible to identify much more rapidly the genes affected in mutant strains [33].

Here we report our identification of 24 conditional mutants in thirteen different essential *C. elegans* loci. To further promote the use and isolation of conditional mutations in essential *C. elegans* genes, we have surveyed this collection of new conditional mutants for essential gene requirements during both larval and early embryonic development, and we have determined whether all are fast or slow acting. We also report the mutations responsible for conditional lethality for most of these alleles, and whether the affected residues are conserved in other organisms.

Results

Over the past several years, using chemical mutagenesis of egg-laying defective *lin-2(-)* mutants with either ethyl methanesulfonate or ethyl nitrosourea, we have isolated conditional mutations in multiple essential *C. elegans* genes that already had been characterized using either mutant alleles or RNAi to reduce gene function. Here we report our identification of 24 conditional mutations in thirteen different essential genes, and an analysis of the conditional nature of the mutations. Most of these mutations were mapped with traditional methods, using both visible markers and individually amplified Single Nucleotide Polymorphisms (SNPs) to score meiotic recombination events. The affected loci were then identified using both complementation tests with previously identified alleles, and DNA sequencing of candidate genes in regions to which the mutations were mapped. More recently, we have begun to take advantage of next generation Illumina DNA sequencing based methods to greatly accelerate the pace at which we can identify the affected genes in mutants isolated after mutagenesis of nematode populations. In the following sections, we describe the conditional mutations we have characterized for each affected locus.

α- and β-Tubulin Mutations

Microtubules are polymers of α- and β-tubulin and are essential for multiple cellular activities, including meiotic and mitotic spindle function. In *C. elegans* embryos there are two functionally redundant α-tubulin genes, *tba-1* and *tba-2*, and also two functionally redundant β-tubulin genes, *tbb-1* and *tbb-2*. While reducing the function of any one gene with RNAi does not result in penetrant phenotypes, reducing the function of either gene pair simultaneously with RNAi results in severe meiotic and mitotic spindle defects and embryonic lethality [34,35]. In addition, we have previously identified conditional, semi-dominant mutations in *tba-1* and *tbb-2* that appear to destabilize microtubules and cause highly penetrant embryonic lethality when adult worms are raised at the restrictive temperature of 26 °C. We have now identified one new *tba-1* mutant, *or594* sd,ts, and one new *tbb-2* allele, *or600* sd,ts. Each of the alleles is semi-dominant (Table 1), as expected given the redundancy of the two gene pairs. We used genetic crosses to place the *or594* ts and *or600* ts alleles in trans to the previously identified alleles *tba-1(or346* ts*)* and *tbb-2(or362* ts*)*, respectively. The progeny of both *or594* ts*/tba-1(or346* ts*)* and *or600* ts*/tbb-2(or362* ts*)* worms exhibited fully penetrant embryonic lethality (data not shown). This is in contrast to the partially penetrant embryonic lethality observed when any of these alleles

Table 1. Embryonic lethality of the TS mutants.

Gene	Allele	Homozygote Embryonic Viability (15°C)	Homozygote Embryonic Viability (26°C)	Heterozygote Embryonic Viability (26°C)
dnc-1	*or404*	98.6%, *n* = 435	0.0%, *n* = 226	99.3%, *n* = 365
dnc-1	*or676*	18.7%, *n* = 626	1.62%, *n* = 747	88.6%, *n* = 474
dnc-4	*or618*	92.7%, *n* = 236	12.7%, *n* = 259	97.7%, *n* = 342
dnc-4	*or633*	99.4%, *n* = 486	3.15%, *n* = 444	77.0%, *n* = 364
lit-1	*or393*	95.6%, *n* = 471	1.55%, *n* = 554	99.1%, *n* = 374
mei-1	*or642*	97.3%, *n* = 1013	0.25%, *n* = 1329	98.5%, *n* = 506
mei-1	*or646*	78.8%, *n* = 438	0.40%, *n* = 1135	98.5%, *n* = 613
mex-1	*or286*	53.1%, *n* = 675	3.4%, *n* = 1327	93.1%, *n* = 249
par-2	*or373*	99.6%, *n* = 282	2.0%, *n* = 251	not tested
par-2	*or539*	94.8%, *n* = 194	42.1%, *n* = 554	97.0%, *n* = 371
par-2	*or640*	98.7%, *n* = 230	0.0%, *n* = 318	89.7%, *n* = 226
plk-1	*or683*	62.3%, *n* = 630	0.80%, *n* = 424	97.8%, *n* = 383
rsa-1	*or598*	99.8%, *n* = 444	1.66%, *n* = 543	100%, *n* = 766
spd-2	*or293*	87.8%, *n* = 245	0.0%, *n* = 341	99.7%, *n* = 378
spd-2	*or493*	95.6%, *n* = 298	1.51%, *n* = 265	100%, *n* = 603
spd-2	*or454*	99.0%, *n* = 412	30.0%, *n* = 410	99.3%, *n* = 412
spd-2	*or655*	58.3%, *n* = 518	0.26%, *n* = 388	98.8%, *n* = 345
sur-6	*or550*	72.8%, *n* = 556	16.0%, *n* = 362	96.1%, *n* = 385
tba-1	*or594*	88.5%, *n* = 278	0.00%, *n* = 402	83.9%, *n* = 261
tbb-2	*or600*	99.1%, *n* = 551	0.81%, *n* = 745	58.4%, *n* = 294
zyg-1	*or278*	78.6%, *n* = 1091	0.0%, *n* = 685	98.7%, *n* = 236
zyg-1	*or297*	93.8%, *n* = 697	0.38%, *n* = 529	99.6%, *n* = 275
zyg-1	*or409*	99.5%, *n* = 411	0.0%, *n* = 396	96.1%, *n* = 233
zyg-1	*or1018*	97.8%, *n* = 276	0.0%, *n* = 407	96.3%, *n* = 246

doi:10.1371/journal.pone.0016644.t001

were in trans to a wild-type copy of the corresponding gene (Table 1; [34,35]), consistent with our conclusion that *or594* ts and *or600* ts are *tba-1* and *tbb-2* alleles, respectively. As shown in Figure 1, we see penetrant defects in embryos produced by homozygous *tba-1(or594* ts*)* and by homozygous *tbb-2(or600* ts*)* mutant worms raised at 26°C from the L4 stage to adulthood (hereafter called mutant embryos). As reported for other conditional and semi-dominant mutations in *tba-1* and *tbb-2*, we observed defects in meiotic spindle function, pronuclear migration, nuclear centrosomal complex (NCC) centration and rotation, mitotic spindle positioning and size, chromosome segregation and cytokinesis during the first mitotic cell cycle (Fig. 1A). Although the new *tba-1(or594* sd,ts*)* mutant and a previous allele, *tba-1(or346* sd,ts*)*, were isolated in different screens, the mutations are identical and change the highly conserved serine at position 377 to phenylalanine (Fig. 1B, Table 2). The mutation in *tbb-2(or600* sd,ts*)* changes a highly conserved glycine at amino acid 140 to a glutamic acid (Fig. 1B, Table 2).The phenotypes were similar to other dominant tubulin alleles but are not as severe as RNAi-mediated co-depletion of either gene pair, and thus represent an approach to disrupt microtubule function less severely than co-depleting either of the gene pairs [34,35]. The *tba-1(or594* sd,ts*)* mutant showed highly penetrant defects when shifted to the restrictive temperature for long (5–8 hours) or short (~1 minute) upshifts, while the *tbb-2(or600* sd,ts*)* mutant showed penetrant defects only after long upshifts (Fig. 1C and Table 3). Shifting *tba-1(or594* sd,ts*)* mutants to the restrictive temperature at the L1 larval stage resulted in mostly fertile worms but about 20% were sterile, while similar shifts with *tbb-2(or600* sd,ts*)* mutants resulted in adult worms that were fertile but produced small broods (Table 4).

Protein phosphatase 2A mutants

Protein phosphatase 2A is composed of a catalytic subunit and regulatory subunits known as B, B′, and B′′. The regulatory subunits provide targeting specificity thereby linking the catalytic subunit to various protein substrates throughout the cell cycle. SUR-6 is the B′ subunit in *C. elegans* and has known functions during embryonic and vulval development [36,37]. We have identified a recessive conditional mutation in *sur-6, or550* ts. The *sur-6(or550* ts*)* mutant embryos produced after shifting homozygous L4 larvae to the restrictive temperature exhibited small male pronuclei, defects in NCC centration, and chromosome segregation defects during mitosis in the one-cell embryo (called P_0), and the posterior P_1 cell in 2-cell stage embryos often divided before its anteriorly positioned sister, called AB (Fig. 2A, and as reported previously for a different allele of *sur-6*, (*sv30*) [36]). In genetic crosses, *sur-6(or550* ts*)* failed to complement *sur-6(sv30)* (data not shown). The amino acid alteration in *sur-6(or550* ts*)* changes a highly conserved tryptophan to arginine at position 140 (Fig. 2B). We could not determine if the allele was fast-acting, even though some phenotypes were observed after short upshifts (Fig. 2C), because of significant embryonic lethality at the permissive temperature (Table 1).

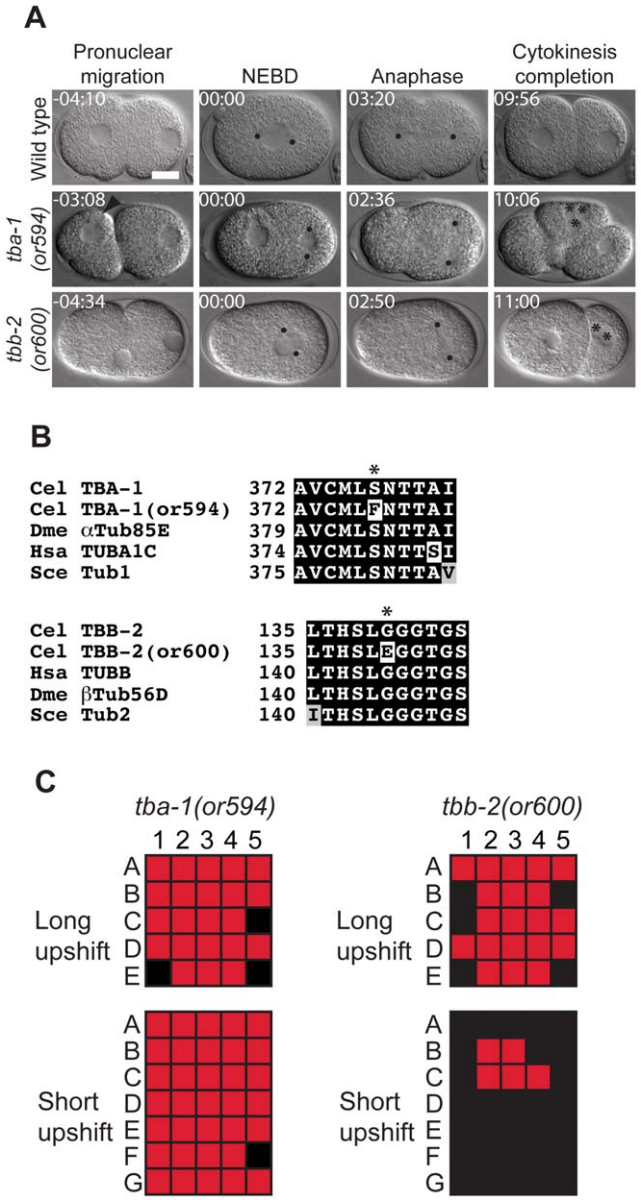

Figure 1. *tba-1* and *tbb-2* tubulin mutants. A. Differential interference contrast (DIC) time-lapse images of wild-type, *tba-1(or594* ts*)*, and *tbb-2(or600* ts*)* embryos. In the two tubulin mutants the P_0 spindle often is positioned transverse to the anterior posterior axis, and daughter cells contained multiple nuclei. The *tba-1(or594* ts*)* embryo was from a~1 min. upshift and the *tbb-2(or600* ts*)* embryo was shifted to the restrictive temperature for 8 hours. Black dots represent centrosomes/spindle poles, asterisks denote multiple nuclei per cell, and the arrowhead indicates a second maternal pronucleus. Times in min:sec are given relative to nuclear envelope breakdown (NEBD). Scale bar, 10 μm. B. Amino acid alterations in the two mutants. Asterisks indicates the changed residues. Homologous proteins are aligned below the *C. elegans* protein. C. Defect maps for individual embryos observed during time-lapse recordings; embryos are listed on the left and phenotypes are listed on the top: 1; pronuclei meet prior to NEBD, 2; Nuclear centrosomal complex centration, 3; Nuclear centrosomal complex rotation, 4; spindle alignment, 5; one nucleus per cell at two cell stage. In the long upshifts, hermaphrodites were transferred to the restrictive temperature for 5–8 hours. In the short upshifts, embryos were harvested from hermaphrodites grown at 15°C and immediately mounted on agar pads for imaging, which took about 1 minute. Red color indicates a defective trait, black color represents the lack of a defect.
doi:10.1371/journal.pone.0016644.g001

The PP2A B′′ subunit is encoded by *rsa-1* in *C. elegans* [38]. We identified one new recessive allele of *rsa-1*, *or598* ts. Like previously characterized alleles or *rsa-1(RNAi)* knockdown, *rsa-1(or598* ts*)* mutant embryos showed multiple defects in the one-cell embryo including defective NCC centration and rotation, small spindles, and chromosome segregation defects (Fig. 3A). *rsa-1(or598* ts*)* is the only TS allele for *rsa-1*, with a conserved aspartic acid changed to glycine at position 319 (Fig. 3B). The *rsa-1* mutant was fast-acting for many of the phenotypes (Fig. 3C and Table 3), and L1 larval upshift resulted in sterile adults (Table 4).

Dynactin mutants

Dynactin is a protein complex that simultaneously binds both microtubules and cytoplasmic dynein [39]. Because dynactin cross-links dynein and microtubules, it increases dynein motor processivity. We isolated two *dnc-1* alleles, *or404* ts and *or676* ts, and two new *dnc-4* alleles, *or618* ts and *or633* ts. All of the dynactin mutants show similar microtubule-related defects in one-cell embryos, as previously reported for *dnc-1* and *dnc-2* using RNAi depletion [40]. Instead of the nuclear-centrosomal complex (NCC) centering in the embryos after meeting, the NCC remains in the posterior in the dynactin mutants. In addition, the NCC fails to rotate causing the P_0 spindle to assemble transverse to the anterior-posterior embryonic axis (Fig. 4A). *dnc-1(or404* ts*)* displayed a somewhat weaker cellular phenotype than the other three *dnc* alleles (Fig. 4C) and, interestingly, *dnc-1(or676* ts*)* and *dnc-4(or633* ts*)* were either semi-dominant or haploinsufficient (Table 1), while the other two *dnc* alleles appeared to be recessive. In genetic crosses, *dnc-1(or404* ts*)* failed to complement *dnc-1(or676* ts*)*, and *dnc-4(or618* ts*)* failed to complement *dnc-4(or633* ts*)* (data not shown). Although *dnc-1(or404* ts*)* was previously characterized [41,42], we have more extensively documented the phenotypes here. No alleles of *dnc-4* have been previously reported nor has it been extensively characterized in *C. elegans*. The *dnc-1(or404* ts*)* allele changes amino acid 1237 from an asparagine to a cysteine. *dnc-1(or676* ts*)* has two changes: one at position 452 (leucine to proline) and the other at position 1247 (valine to leucine). *dnc-4(or618* ts*)* substitutes valine for a glycine at position 359 and *dnc-4(or633* ts*)* has an altered splice donor site after the first exon (G to A) at nucleotide 604 in the unspliced RNA molecule. The *dnc-1(or404* ts*)* and *dnc-4(or633* ts*)* mutants appeared to be fast-acting (Fig. 4C and Table 3). Finally, in tests where L1 larvae were raised to adulthood at the restrictive temperature, we found that *dnc-1(or404* ts*)* and *dnc-4(or618* ts*)* worms displayed egg-laying defects, *dnc-1(or676* ts*)* worms were sterile or produced small numbers of progeny, while *dnc-4(or633* ts*)* worms also produced reduced numbers of progeny (Table 4).

mei-1/Katanin mutants

The meiotic spindles in the oocytes of most animals are smaller than mitotic spindles. In *C. elegans*, meiosis I and II spindles are about 8-fold smaller than the first embryonic mitotic spindle and are acentriolar. The length of microtubules during *C. elegans* meiosis are controlled in part by a katanin, a heterodimeric protein complex composed of MEI-1 and MEI-2 [43,44]. *mei-1* encodes the AAA ATPase-containing catalytic subunit and *mei-2* encodes the targeting subunit [45]. Katanin is widely conserved and functions to shorten microtubules by severing them [46]. We isolated two recessive mutants in *mei-1*, *or642* ts and *or646* ts. The new *mei-1* mutants disrupt female meiotic spindle function and produce one-cell stage embryos with large misshapen polar bodies and a variable number of maternal pronuclei (range = 0–9; see Fig. 5A, B). Similar phenotypes have been described previously for other alleles [47], and both *mei-1(or642* ts*)* and *mei-1(or646* ts*)*

Table 2. Sequence alterations in the TS mutants.

Gene	Allele	Transcript[1]	Codon(s) mutated[1]	Amino acid change[1]	Nucleotide change[1]	Transcript nucleotide (spl/unspl)[1,2]
dnc-1	*or404*	ZK593.5	1237	R>C	C>T	3709 (spl)
dnc-1	*or676*[3]	ZK593.5	452	L>P	T>C	1355 (spl)
dnc-1	*or676*[3]	ZK593.5	1247	V>L	G>C	3739 (spl)
dnc-4	*or618*	C26B2.1	359	V>G	T>G	1076 (spl)
dnc-4	*or633*	C26B2.1	-	-	G>A	604 (unspl)
lit-1	*or393*	W06F12.1a	331	I>F	A>T	991 (spl)
mei-1	*or642*	T01G9.5a.1	202	K>Q	A>C	604 (spl)
mei-1	*or646*	T01G9.5a.1	202	K>Q	A>C	604 (spl)
mex-1	*or286*	W03C9.7.1	13	Q>STOP	C>T	37 (spl)
plk-1	*or683*	C14B9.4a.1	547	M>K	T>A	1640 (spl)
rsa-1	*or598*	C25A1.9a	319	D>G	A>G	956 (spl)
spd-2	*or293*	F32H2.3.1	573	G>S	G>A	1717 (spl)
spd-2	*or493*	F32H2.3.1	551	R>H	G>A	1652 (spl)
spd-2	*or454*	F32H2.3.1	-	-	G>A	2175 (unspl)
spd-2	*or655*	F32H2.3.1	189–270	Deletion	Deletion	565–810Δ spl)
sur-6	*or550*	F26E4.1	140	W>R	T>C	418 (spl)
tba-1	*or594*	F26E4.8.1	377	S>F	C>T	1130 (spl)
tbb-2	*or600*	C36E8.5.1	140	G>E	G>A	419 (spl)
zyg-1	*or278*	F59E12.2.1	354	P>S	C>T	1060 (spl)
zyg-1	*or297*	F59E12.2.1	652	D>N	G>A	1954 (spl)
zyg-1	*or409*	F59E12.2.1	670	D>N	G>A	2008 (spl)
zyg-1	*or1018*	F59E12.2.1	498	V>A	T>C	1493 (spl)
par-2	*or373*	F58B6.3a	71	C>Y	G>A	212 (spl)

[1]Transcripts, positions, and sequences are from the WS210 referential release of Wormbase.
[2]Positions are provided for either spiced (spl) or unspliced (unspl) transcripts.
[3]*dnc-1(or676)* was a double mutant.
doi:10.1371/journal.pone.0016644.t002

failed to complement the previously identified allele *mei-1(b284)* (data not shown). We also observed multiple nuclei per two-cell blastomere, indicating chromosome segregation anomalies (which were possibly indirectly due to meiotic spindle defects), as well as occasional NCC rotation defects and transverse P_0 spindles. The *mei-1(or642* ts*)* and *mei-1(646* ts*)* alleles each contain the same mutation even though they were isolated from different mutagenized nematode populations. The mutation in each changes a highly conserved lysine to glutamine at codon 202 and causes fast-inactivation of MEI-1 function (Fig. 5B, C, and Table 3). We did not find any role for *mei-1* during development after embryogenesis (Table 4).

spd-2 mutants

Centrosomes are complex structures composed of centrioles surrounded by pericentriolar material that nucleates microtubules during mitotic spindle assembly and in other contexts [48]. SPD-2 is a centrosomal component required for both centriole duplication and maturation of the pericentriolar material [49,50,51]. We isolated four new recessive alleles of *spd-2* that cause a variety of centrosomal and microtubule-related defects, and all four alleles failed to complement the previously identified allele *spd-2(or188* ts*)*[49] (data not shown). In one-cell embryos, we often observed that pronuclei met in the cell center instead of toward the posterior, NCC rotation and spindle assembly were absent, cytokinesis often failed, and chromosome segregation was defective (Fig. 6A). One of the *spd-2* alleles was fast-acting, *or293* ts, while *or493* ts and *or454* ts mutant embryos showed weak and only partially penetrant defects when shifted to the restrictive temperature for 1 minute (Fig. 6C and Table 3). Two of the *spd-2* mutations were single amino acid substitutions: *spd-2(or293* ts*)* changes a glycine at position 573 with a serine while *spd-2(or493* ts*)* replaces an arginine at position 551 with a histidine (Fig. 6B and Table 2). *spd-2(or454* ts*)* had a mutation in the last nucleotide of the fifth intron: position 2175 of the unspliced transcript was changed from a guanine to an adenine (Fig. 6B and Table 2), and this mutant produced a large percentage of viable embryos at the nonpermissive temperature (Table 1). The *spd-2* protein encoded by *spd-2(or655* ts*)* contains an in-frame deletion that removes amino acids 189–270, and this mutant produces only 58% viable embryos at 15°C. *spd-2(or293* ts*)* also resulted in sterile hermaphrodites with protruding vulvas when raised to adulthood at the restrictive temperature, and L1-upshifted *spd-2(or493* ts*)* worms produced small broods (Table 4).

zyg-1 mutants

ZYG-1 is a polo-related kinase homologous to vertebrate SAK/PLK4 [52] that localizes to centrioles and is required for centriole duplication [53]. During fertilization, a single sperm cell provides two centrioles as well as paternal DNA to embryos, and thus embryos lacking maternal *zyg-1* function successfully proceed to the two-cell stage. However, during the AB and P_1 cell divisions,

Table 3. Determination if the TS mutations are potentially fast-acting.

Gene	Allele	Potentially Fast-acting[1]
dnc-1	*or404*	Yes
dnc-1	*or676*	Unclear[3]
dnc-4	*or618*	Yes
dnc-4	*or633*	Yes
lit-1	*or393*	Not tested
mei-1[2]	*or642*	Yes
mei-1[2]	*or646*	Yes
mex-1	*or286*	Not tested
par-2[2]	*or373*	Yes
par-2[2]	*or539*	Yes
par-2[2]	*or640*	Yes
plk-1	*or683*	Unclear[3]
rsa-1	*or598*	Yes
spd-2	*or293*	Yes
spd-2	*or493*	Unclear[4]
spd-2	*or454*	Unclear[4]
spd-2	*or655*	Unclear[3]
sur-6	*or550*	Unclear[3]
tba-1	*or594*	Yes
tbb-2	*or600*	No
zyg-1[2]	*or278*	No
zyg-1[2]	*or297*	Yes
zyg-1[2]	*or409*	Yes
zyg-1[2]	*or1018*	No

[1]We determined if an allele was potentially fast-acting in the following manner: We mounted embryos produced at 15°C on microscope slides and immediately made time-lapse videomicrographs at a room maintained at 24°C. If defects similar to those observed after long temperature shifts were found in at least 20% of the embryos and if there was little embryonic lethality at 15°C, we conclude that the allele may be fast-acting. We have labeled these cases as "Yes". However, if there was significant embryonic lethality at 15°C, we cannot conclude that the presence of cellular defects after short upshifts is due to the upshift or to defects that occur even at 15°C. We have labeled these cases as "Unclear".

[2]For *mei-1, par-2,* and *zyg-1*, we incubated mutant worms at 26°C for 30 minutes prior to imaging (instead of the usual~1 min. upshift) because the gene products appeared to be required prior to when we started our imaging (pronuclear migration).

[3]High lethality at the permissive temperature precludes making a determination.

[4]The low penetrance of severe defects precludes making a determination.

doi:10.1371/journal.pone.0016644.t003

Table 4. The phenotypes of the TS mutants when grown at the restrictive temperature from the L1 larval stage.

Gene	Allele	L1 upshift phenotype[1]
dnc-1	*or404*	Egl/Emb
dnc-1	*or676*	Ste/Sb/Emb
dnc-4	*or618*	Egl/Emb
dnc-4	*or633*	Sb/Emb
lit-1	*or393*	Emb
mei-1	*or642*	Emb
mei-1	*or646*	Emb
mex-1	*or286*	Ste/Sb/Emb
par-2	*or373*	Emb
par-2	*or539*	Emb
par-2	*or640*	Ste
plk-1	*or683*	Ste/Pvl
rsa-1	*or598*	Ste
spd-2	*or293*	Ste/Pvl
spd-2	*or493*	Sb/Emb
spd-2	*or454*	Emb
spd-2	*or655*	Emb
sur-6	*or550*	Emb
tba-1	*or594*	Emb/Ste
tbb-2	*or600*	Sb/Emb
zyg-1	*or278*	Sb/Emb
zyg-1	*or297*	Emb
zyg-1	*or409*	Sb/Emb
zyg-1	*or1018*	Sb/Emb

[1]We determined the L1 upshift phenotype by plating hypochlorite-synchronized L1 larvae and incubating them at 26°C until they reached adulthood. Abbreviations: Egl: egg laying-defective, Emb: embryonic lethal, Pvl: protruding vulva, Sb: small broods, Ste: sterile.

doi:10.1371/journal.pone.0016644.t004

zyg-1 mutants form monopolar spindles because the mutant maternal ZYG-1 protein is incapable of supporting centriole duplication [53]. We isolated four new recessive alleles of *zyg-1* that cause monopolar spindles and failed mitosis in the AB and P_1 cells (Fig. 7A and Table 1). Each of the *zyg-1* alleles alters amino acids in the C-terminal domain that appears to be nematode-specific: *zyg-1(or278* ts*)* changes a proline to a serine at codon 354, *zyg-1(or297* ts*)* changes an aspartic acid to asparagine at codon 652, zyg-*1(or409* ts*)* changes a aspartic acid to an asparagine at codon 670, and *zyg-1(or1018* ts*)* changes a valine to an alanine at codon 498 (Fig. 7B and Table 2). *zyg-1(or297* ts*)* and *zyg-1(or409* ts*)* appeared to be fast-acting as a 30 minute upshift resulted in penetrant defects (Fig. 7C). With the exception of *zyg-1(or297* ts*)*, each of the new *zyg-1* TS mutants produced small broods when shifted to the restrictive temperature at the L1 larval stage (Table 4).

A plk-1 mutant

PLK-1 is a polo-like kinase that is required for meiotic spindle function, nuclear envelope breakdown, embryonic polarity, and asynchronous cell divisions in the two-cell embryo [54,55,56,57]. For some of these functions, *plk-1* appears to be partially redundant with *plk-2* [56]. We isolated one new recessive allele of *plk-1*, *or683 ts*, which appears to only partially reduce gene function as the most penetrant phenotypes we observed at the restrictive temperature were mis-oriented (transverse) P_0 spindles and binucleate cells at the two-cell stage (Figure 8). The *plk-1(or683 ts)* allele failed to complement the non-conditional sterile deletion allele *plk-1(ok1787)* (data not shown). Otherwise, meiotic and mitotic spindle function appeared normal. We observed penetrant defects in *plk-1* embryos after short (~1 minute) upshifts, but as the strain produces 38% inviable embryos at the permissive temperature, we cannot conclude that it is fast-acting (Tables 1 and 3). The *plk-1(or698 ts)* mutation changes a methionine to a lysine at codon 547 that is invariably hydrophobic in various organisms (Fig. 8B). Shifting L1 larvae to the restrictive temperature resulted in sterile worms with protruding vulvae

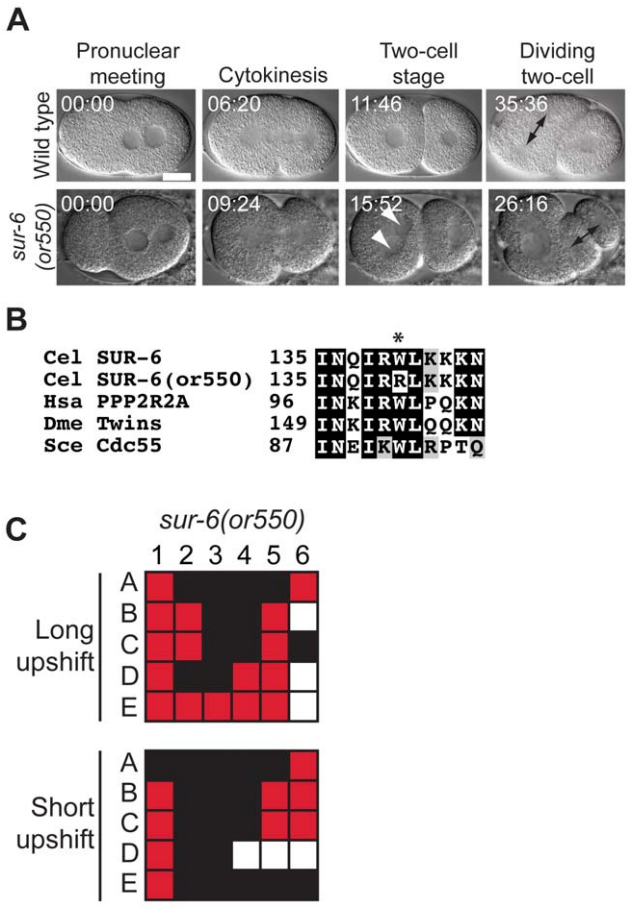

Figure 2. A *sur-6* mutant. A. DIC time-lapse images of wild-type and *sur-6(or550* ts*)* embryos. In the *sur-6* mutant the male pronucleus is small, the AB cell contains two nuclei, and the P_1 cell begins mitosis before the AB cell. The *sur-6(or550* ts*)* embryo was shifted to the restrictive temperature for ~1 min. prior to imaging. White arrowheads denote multiple nuclei per cell, and the arrows in the last panels indicate the first mitotic spindle at the two cell stage. Times in min:sec are given relative to pronuclear meeting. Scale bar, 10 μm. B. Amino acid alteration in the mutant. Asterisk indicates the changed residue. Homologous proteins are aligned below the *C. elegans* protein. C. Defect maps for individual embryos observed during time-lapse recordings. In this and all subsequent figures, embryos are listed on the left and phenotypes are listed on the top: 1; Male pronuleus normal size, 2; Nuclear centrosomal complex centration, 3; spindle alignment, 4; successful cytokinesis, 5; one nucleus per cell at two cell stage, 6; AB divides first at two cell stage. In the long upshifts, hermaphrodites were transferred to the restrictive temperature for 5–8 hours. In the short upshifts, embryos were harvested from hermaphrodites grown at 15°C and immediately mounted on agar pads for imaging, which took ~1 min. In this and all subsequent figures, red color indicates a defective trait, black color represents the lack of a defect, and white indicates that the trait was not visible in the recording.
doi:10.1371/journal.pone.0016644.g002

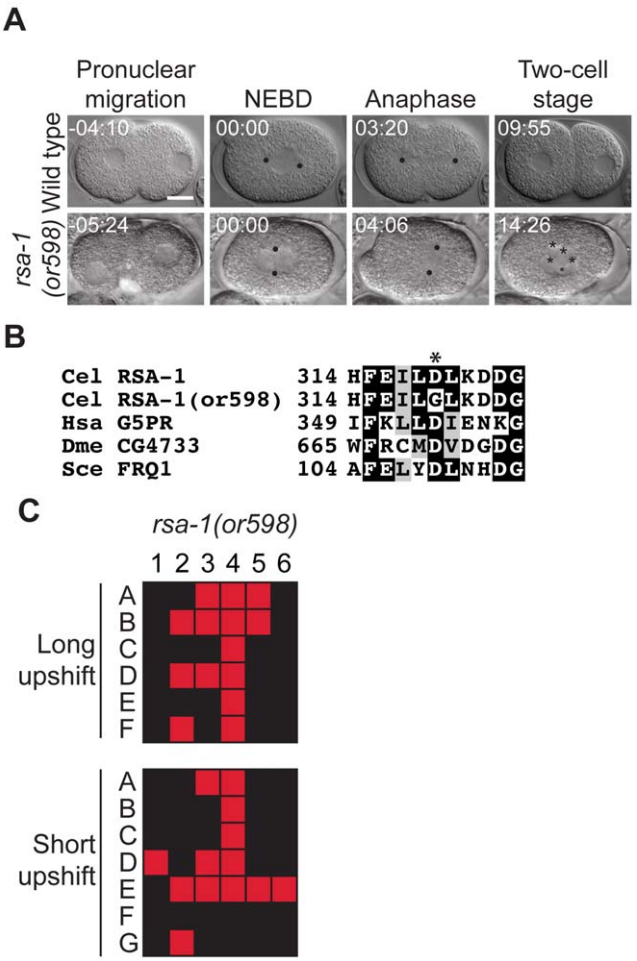

Figure 3. An *rsa-1* mutant. A. DIC time-lapse images of wild-type and *rsa-1(or598* ts*)* embryos. In the *rsa-1* mutant the nuclear centrosomal complex (NCC) failed to rotate and a small transverse P_0 spindle assembled, cytokinesis failed, and multiple nuclei were present at the two cell equivilent stage. The *rsa-1(or598* ts*)* embryo was shifted to the restrictive temperature for~1 min. prior to imaging. Black dots represent centrosomes/ spindle poles and asterisks denote multiple nuclei per cell at the two cell stage. Times in min:sec are given relative to NEBD. Scale bar, 10 μm. B. Amino acid alteration in the mutant. Asterisk indicates the changed residue. Homologous proteins are aligned below the *C. elegans* protein. C. Defect map for individual embryos observed during time-lapse recordings: embryos are listed on the left and phenotypes are listed on the top: 1; pronuclei meet prior to NEBD, 2; Nuclear centrosomal complex centration, 3; Nuclear centrosomal complex rotation, 4; spindle size, 5; successful cytokinesis, 6; one nucleus per cell at two cell stage. In the long upshifts, hermaphrodites were transferred to the restrictive temperature for 5–8 hours. In the short upshifts, embryos were harvested from hermaphrodites grown at 15°C and immediately mounted on agar pads for imaging, which took ~1 min.
doi:10.1371/journal.pone.0016644.g003

(Table 4). Interestingly, no other *plk-1* alleles have been reported (Table 5).

par-2 mutants

par-2 is required for anterior-posterior polarity in the one-cell zygote and encodes a RING finger protein [58,59,60]. We isolated three new recessive *par-2* mutants that disrupt zygote polarity; all three alleles failed to complement the previously identified allele *par-2(lw32)* (data not shown). In two-cell embryos the lack of polarity was revealed by blastomeres having equal size that entered mitosis at the same time, in contrast to wild-type embryos that display asymmetric AB and P_1 cell sizes and timing of mitotic entry (Fig. 9A). *par-2(or539 ts)* had low penetrance cellular defects after both short and long upshifts, consistent with the fact that it produces a high percentage of viable embryos at the restrictive temperature (Table 1). All of the alleles appeared to be fast-acting, although for *par-2(or373 ts)* and *par-2(or640 ts)* the penetrance of defects observed after short upshifts was lower than seen after long upshifts (Fig. 9B, Table 3). We found that *par-2(or373 ts)* contained a cysteine to tyrosine change at codon 71 (Fig. 9C and Table 2).

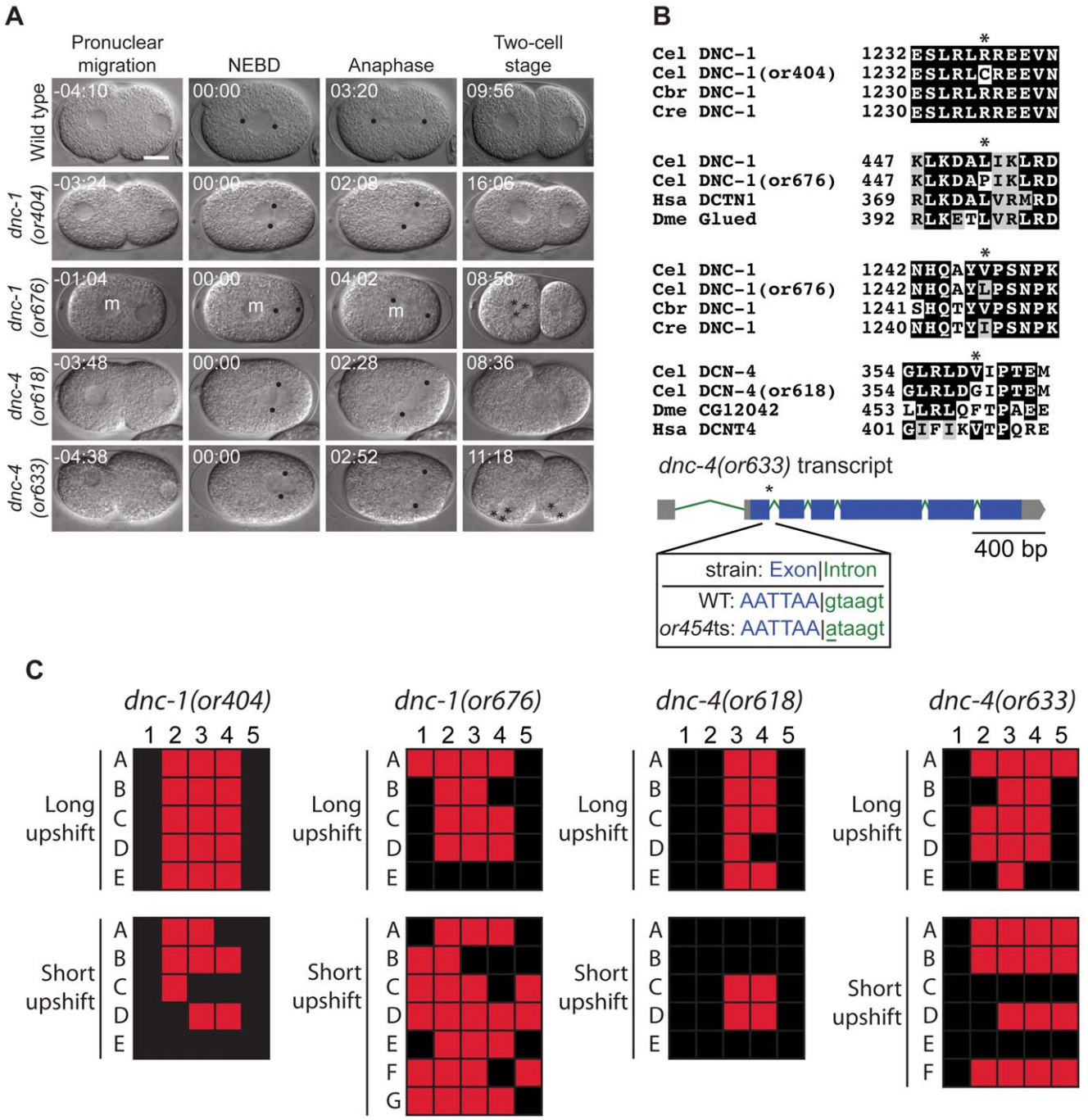

Figure 4. Dynactin mutants. A. DIC time-lapse images of wild-type, *dnc-1(or404* ts*), dnc-1(or676* ts*), dnc-4(or618* ts*), and dnc-4(or633* ts*)* embryos. In the dynactin mutants the NCC often failed to centrate and rotate, the P_0 spindle was oriented transverse to the anterior posterior axis, and multiple nuclei were present per cell at the two cell stage. The *dnc-1(or404* ts*)* embryo was obtained from a hermaphrodite shifted to the restrictive temperature for 8 hours, the *dnc-1(or676* ts*)* and *dnc-4(or633* ts*)* embryos were shifted to the restrictive temperature for ~1 min. prior to imaging, and the *dnc-4(or618* ts*)* embryo was obtained from a hermaphrodite shifted to the restrictive temperature for 7 hours. Black dots represent centrosomes/spindle poles, asterisks denote multiple nuclei per cell, and the ''m'' denotes the maternal pronucleus that did not meet the male pronucleus prior to NEBD. Times in min:sec are given relative to nuclear envelope breakdown (NEBD). Scale bar, 10 μm. B. Sequence alterations in the mutants. Asterisks indicate the changed residues (or nucleotide for *dnc-4(or633* ts). Homologous proteins are aligned below the *C. elegans* proteins. *dnc-4(or633* ts*)* contains a mutation in an intron that may affect RNA splicing. C. Individual embryos observed during time-lapse recordings: embryos are listed on the left and phenotypes are listed on the top: 1; pronuclei meet prior to NEBD, 2; Nuclear centrosomal complex centration, 3; Nuclear centrosomal complex rotation, 4; spindle alignment, 5 one nucleus per cell at two cell stage. In the long upshifts, hermaphrodites were transferred to the restrictive temperature for 5–8 hours. In the short upshifts, embryos were harvested from hermaphrodites grown at 15°C and immediately mounted on agar pads for imaging, which took ~1 min.

doi:10.1371/journal.pone.0016644.g004

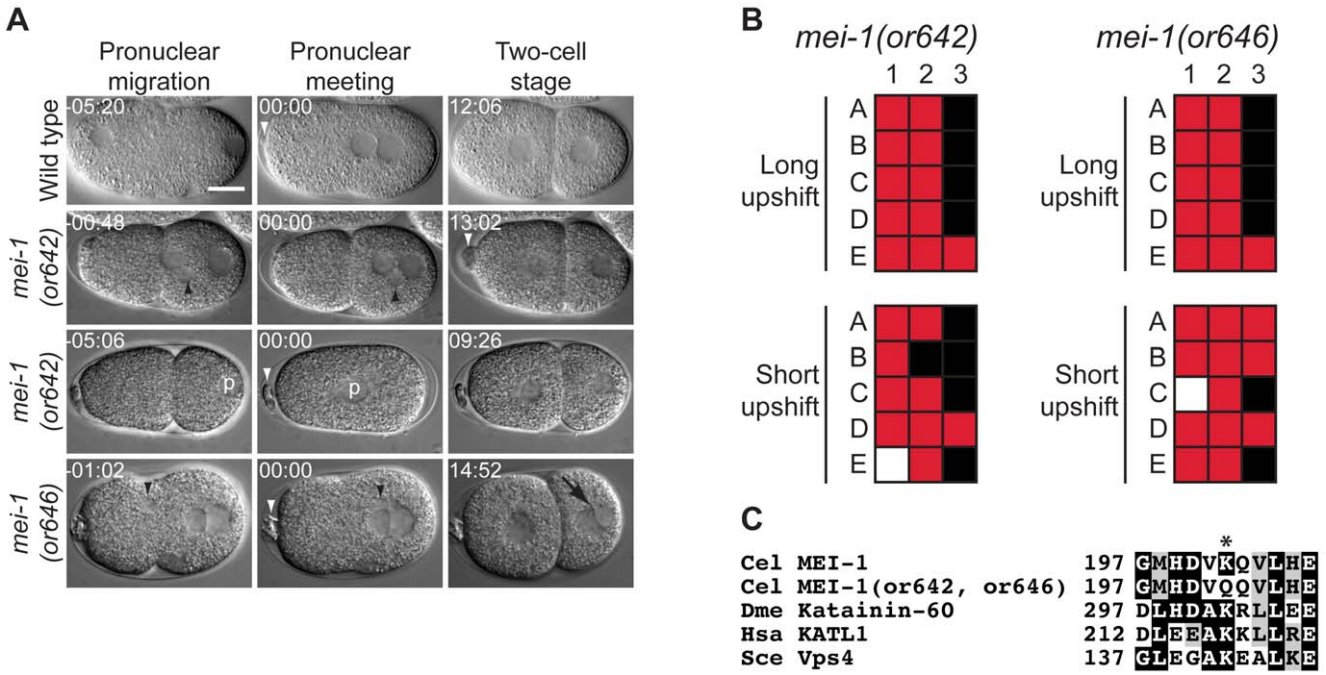

Figure 5. *mei-1* mutants. A. DIC time-lapse images of wild-type, *mei-1(or642* ts*) and mei-1(or646* ts*)* embryos. In the *mei-1* mutants the polar bodies were large and misshapen and embryos contained multiple [top *mei-1(or642* ts*)* embryo and *mei-1(or646* ts*)*] or zero maternal pronuclei (second *mei-1(or642* ts*)* embryo). The two *mei-1(or642* ts*)* embryos were obtained from a hermaphrodite shifted to the restrictive temperature for 30 minutes, the *mei-1(or646* ts*)* embryo was obtained from a hermaphrodite shifted to the restrictive temperature for 7 hours prior to imaging. White arrowheads indicates polar bodies, black arrowheads indicate multiple maternal pronuclei, the black arrow denotes multiple nuclei per cell at the two cell stage, and the "p" refers to the paternal pronucleus in an embryo lacking a maternal pronucleus. Times in min:sec are given relative to nuclear envelope breakdown (NEBD). Scale bar, 10 μm. B. Defect maps of individual embryos observed during time-lapse recordings: embryos are listed on the left and phenotypes are listed on the top: 1; normal polar body size, 2; normal pronuclear number, 3; one nucleus per cell at two cell stage. In the long upshifts, hermaphrodites were transferred to the restrictive temperature for 5–8 hours. In the short upshifts, embryos were harvested from hermaphrodites grown at the restrictive temperature for 30 minutes. C. Amino acid alteration in the mutants. Asterisk indicates the changed residue. Homologous proteins are aligned below the *C. elegans* protein.
doi:10.1371/journal.pone.0016644.g005

Finally, *par-2(or373 ts)* and *par-2(or539 ts)* worms were fertile and produced inviable embryos when grown to adulthood from the L1 larval stage, but the *par-2(or640 ts)* mutant worms were sterile after L1 temperature upshifts (Table 4).

lit-1 and *mex-1* mutants

lit-1 and *mex-1* control embryonic cell fate patterning. LIT-1 is a kinase that controls anterior/posterior daughter cell fates beginning at the 6-cell stage when the ventral-most embryonic cell called EMS divides along the anterior/posterior body axis [61,62,63]. MEX-1 is a zinc finger protein that restricts blastomere identity at the 8-cell stage but also has been shown to affect anterior-posterior polarity at the one-cell stage [64,65,66]. We found one new *lit-1* mutant, *or393 ts* and one new *mex-1* mutant, *or286 ts*, which failed to complement the previously identified alleles *lit-1(or131 ts)* and *mex-1(zu120)*, respectively (data not shown). *lit-1(or393 ts)* hermaphrodites produced embryos that contained fewer intestinal cells, as compared to wild-type worms (not shown). *lit-1(or393 ts)* was recessive (Table 1) and did not exhibit any phenotypes other than embryonic lethality when grown to adulthood at the restrictive temperature from the L1 larval stage (Table 4). We found that codon 331 was changed from an isoleucine to a phenylalanine in *lit-1(or393 ts)* strain (Fig. 10 and Table 2). *mex-1(or286 ts)* hermaphrodites generated embryos that, as reported previously for other alleles, produced a large excess of pharyngeal tissue (data not shown). L1 upshift experiments revealed that *mex-1* worms produced either small broods or were sterile (Table 4). The sequence alteration in the *mex-1(or286 ts)* mutant changed a glutamine at codon 13 to a stop codon (Fig. 10 and Table 2).

Discussion

Most of the effort to investigate essential *C. elegans genes* has thus far focused on gene products that, when defective, exhibit early embryonic cell division defects. However, extending efforts to investigate previously ignored or poorly studied mutant classes is now more appealing with the rapid cloning methods available. These mutant classes include eggshell-defective mutants, sterile or small brood-producing mutants, mutants with delayed progression through S phase, and mutants with normal early embryonic cell divisions but highly penetrant lethality presumably due to defects later in embryogenesis. By first identifying what genes are affected in such mutants, research effort might be more productively focused on conserved genes with important roles in other model systems and in human health.

Most of the mutants we describe here have been studied previously, either by using mutant alleles or RNAi depletion, and the cellular phenotypes we present mirror what has been presented previously. However, these new strains should still prove valuable for the phenotypic analysis of embryos and worms after bypassing the earliest defects, by providing sensitized backgrounds for use in modifier screens, for defining temperature-sensitive periods, and as templates for engineering TS alleles in homologous genes (see

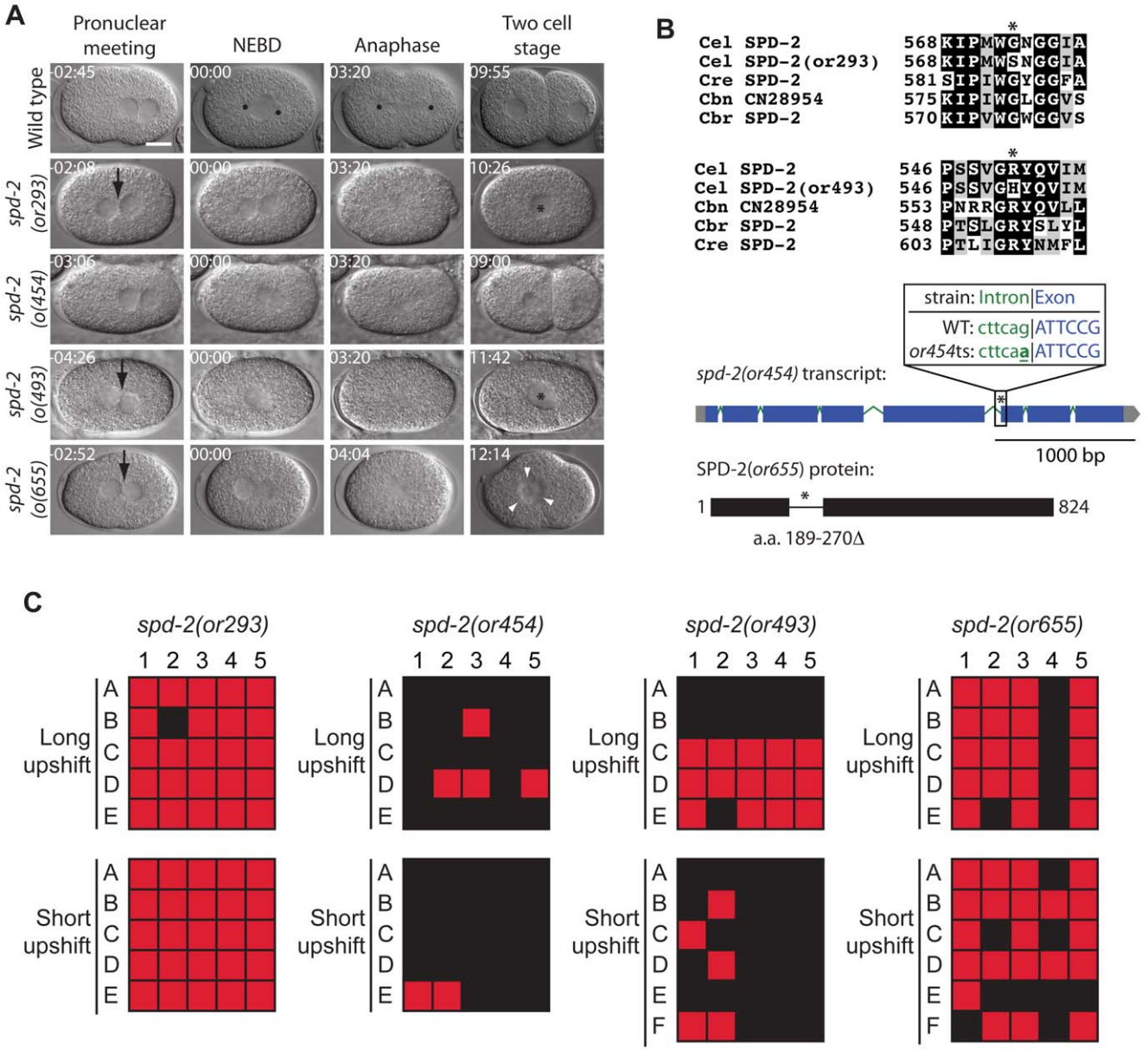

Figure 6. *spd-2* mutants. A. DIC time-lapse images of wild-type, *spd-2(or293* ts*)*, *spd-2(or454* ts*)*, *spd-2(or493* ts*)*, and *spd-2(or655* ts*)* embryos. In the *spd-2* mutants the pronuclei often met in the center, NCC rotation failed, a bipolar spindle failed to assemble, cytokinesis failed, and there were aberrent numbers of nuclei present at the two cell stage. The *spd-2(or293* ts*), spd-2(or454* ts*), and spd-2(or493* ts*)* embryos were obtained from hermaphrodites shifted to the restrictive temperature for 5–6 hours. The *spd-2(or655* ts*)* embryo was obtained from a hermaphrodite shifted to the restrictive temperature for ~1 min prior to imaging. Black arrows indicate instances when pronuclei meet in the center of the embryo, asterisks represent one nucleus present in a two cell stage equivalent embryo, and white arrowheads indicate multiple nuclei. Times in min:sec are given relative to nuclear envelope breakdown (NEBD). Scale bar, 10 μm. B. Sequence alterations in the mutants. Asterisks indicates the changed residues (or nucleotide for *spd-2(or454* ts*)*. Homologous proteins are aligned below the *C. elegans* protein. C. Defect maps for the *spd-2* mutants. Individual embryos observed during time-lapse recordings: embryos are listed on the left and phenotypes are listed on the top: 1; nuclear centrosomal complex centration, 2; nuclear centrosomal complex rotation, 3; bipolar spindle, 4; successful cytokinesis, 5; one nucleus per cell at two cell stage. In the long upshifts, hermaphrodites were transferred to the restrictive temperature for 5–8 hours. In the short upshifts, embryos were harvested from hermaphrodites grown at 15°C and immediately mounted on agar pads for imaging, which took ~1 min.
doi:10.1371/journal.pone.0016644.g006

below). One interesting finding we have made is that fast-acting TS alleles (as defined by our criteria) are not unusual (Table 3). Thirteen of the alleles we have characterized here are potentially fast-acting, and we could not make a determination on six others because of either 1) weak or low penetrance defects or, 2) high lethality at the permissive temperature. In fact, only three mutations were definitively not fast-acting. In future assays, it may be useful to grow worms and conduct rapid upshifts in a room maintained at 15°C by use of a temperature-controlled microscope stage, in order to bypass mounting embryos at room temperature (which would likely allow one to further clarify the "Unclear" determinations in Table 4). The observation that~50% of the conditional mutants we analyzed are potentially fast-acting provides additional incentive to isolate more TS alleles.

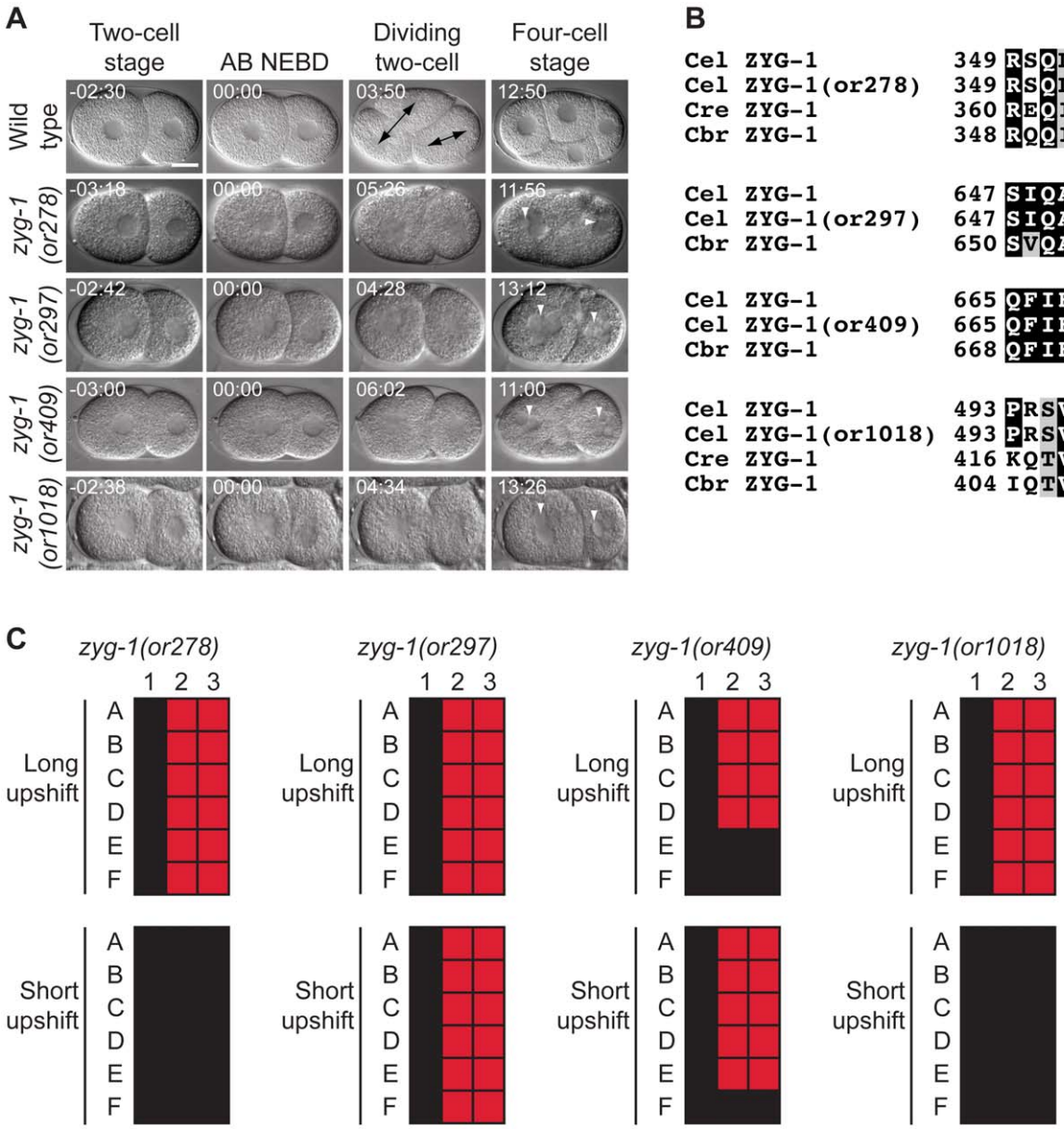

Figure 7. *zyg-1* mutants. A. DIC time-lapse images of wild-type, *zyg-1(or278* ts*)*, *zyg-1(or297* ts*)*, *zyg-1(or409* ts*)*, and *zyg-1(or1018* ts*)* embryos. In the *zyg-1* mutants the two cell stage blastomeres assembled monopolar spindles, cytokinesis failed, and there were multiple nuclei present at the four cell equivilent stage. The *zyg-1(or278* ts*)*, *zyg-1(or409* ts*)*, and *zyg-1(or1018* ts*)* embryos were obtained from hermaphrodites shifted to the restrictive temperature for 5–6 hours. The *zyg-1(or297* ts*)* embryo was obtained from a hermaphrodite shifted to the restrictive temperature for 30 minutes prior to imaging. Black arrows indicate normal bipolar spindles in the wild-type embryo and white arrowheads indicate multiple nuclei present at the four cell equivalent stage. Times in min:sec are given relative to AB nuclear envelope breakdown (NEBD). Scale bar, 10 μm. B. Amino acid alterations in the mutants. Asterisks indicate the changed residues. Homologous proteins are aligned below the *C. elegans* protein. C. Defect maps for the *zyg-1* mutants.Individual embryos observed during time-lapse recordings: embryos are listed on the left and phenotypes are listed on the top: 1; normal two cell embryo, 2; bipolar spindles at two cell stage, 3; one nucleus per cell at four cell stage. In the long upshifts, hermaphrodites were transferred to the restrictive temperature for 5–8 hours. In the short upshifts, embryos were harvested from hermaphrodites grown at the restrictive temperature for 30 minutes.

doi:10.1371/journal.pone.0016644.g007

Of the 13 loci we have described, no genetic alleles have been described for two *(dnc-4 and plk-1)*, while no TS alleles have been described for three others *(mex-1, rsa-1, and sur-6;* see Table 5). Sixteen of the sequenced TS alleles are single mis-sense mutations and another allele, *dnc-1(or676 ts)* has two mis-sense mutations. Two of the TS alleles, *dnc-4(or633 ts)* and *spd-2(or454 ts)*, change nucleotides in introns that likely affect RNA splicing, and interestingly, *dnc-4(or633 ts)* is highly temperature-sensitive while *spd-2(or454 ts)* is less so (Table 1). It would be interesting to test if engineering either of these splice site mutations into other genes would also confer conditional gene function. One of the mutants contains an in-frame deletion, *spd-2(or655 ts)*, while *mex-1(or286 ts)* has a premature stop codon, and both of these mutants produce a substantial fraction of inviable embryos at the permissive temperature (Table 1). As 81% of our TS alleles were mis-sense mutations, searching for mis-sense mutations in mutant genome

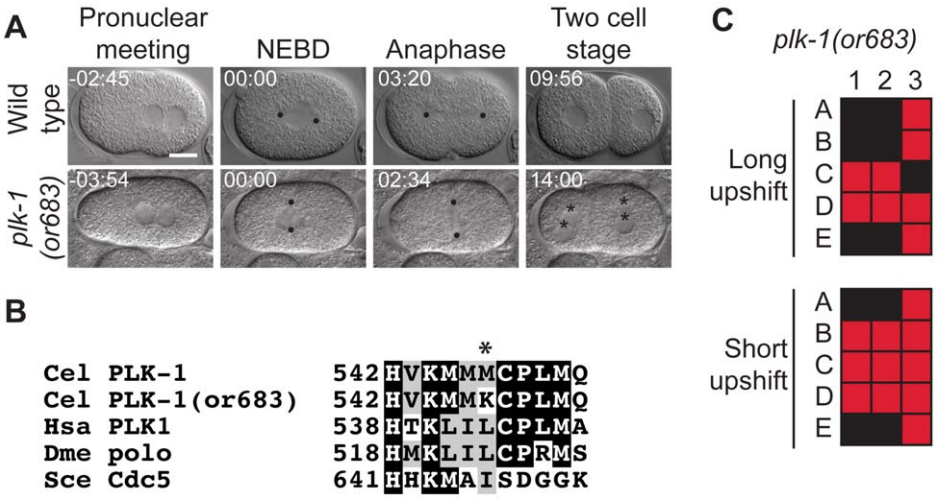

Figure 8. A *plk-1* mutant. A. DIC time-lapse images of wild-type and *plk-1(or683* ts*)* embryos. In the *plk-1* mutant the nuclear centrosomal complex (NCC) failed to rotate, a transverse P_0 spindle assembled, and the daughter blastomeres were binucleate. The *plk-1(or683* ts*)* embryo was obtained from a hermaphrodite shifted to the restrictive temperature for 6 hours prior to imaging. Black dots represent centrosomes/spindle poles and asterisks denote multiple nuclei per cell at the two cell stage. Times in min:sec are given relative to NEBD. Scale bar, 10 μm. B. Amino acid alteration in the mutant. Asterisk indicates changed residue. Homologous proteins are aligned below the *C. elegans* protein. C. Defect map for individual embryos observed during time-lapse recordings, embryos are listed on the left and phenotypes are listed on the top: 1; nuclear centrosomal complex rotation, 2; spindle alignment, 3; one nucleus per cell at two cell stage. In the long upshifts, hermaphrodites were transferred to the restrictive temperature for 5–8 hours. In the short upshifts, embryos were harvested from hermaphrodites grown at 15°C and immediately mounted on agar pads for imaging, which took ~1 min.
doi:10.1371/journal.pone.0016644.g008

exon sequences should lead to finding the causative mutations in most TS mutants. Finally, the amino acid substitutions in nine of the alleles alter residues that are similar (seven of them are identical) in homologous proteins in vertebrates, *Drosophila melanogaster*, and budding yeast. Thus, it may be possible to engineer these changes in other organisms to obtain TS alleles. Eight of the TS alleles alter residues only conserved within nematodes. As a substantial fraction of the TS mutations we have described either do affect widely conserved residues, or are not fast-acting, further efforts to identify additional conditional mutations in even these essential *C. elegans* genes may prove valuable, and TS mutations have yet to be identified for most of the roughly 2500 essential genes present in the *C. elegans* genome.

Materials and Methods

C. elegans strains and culture

Strains were grown under standard laboratory conditions [67]. The temperature sensitive mutants were maintained in a 15°C incubator and shifted to a 26°C incubator to perform temperature upshifts for determining embryonic lethality. Mutants were isolated in a *lin-2(e1309)* background, as previously described [25]. For performing embryonic viability counts, we transferred

Table 5. Summary of the TS mutant loci and comparison of previously available alleles.

Locus	Allele(s) reported in this paper	Previous allele(s) published[1]	Previous TS allele(s) available[1]
dnc-1	*or404, or676*	yes	yes
dnc-4	*or618, or633*	no	no
lit-1	*or393*	yes	yes
mei-1	*or642, or646*	yes	yes
mex-1	*or286*	yes	no
par-2	*or373, or539, or640*	yes	yes
plk-1	*or683*	no	no
rsa-1	*or598*	yes	no
spd-2	*or293, or493, or454, or655*	yes	yes
sur-6	*or550*	yes	no
tba-1	*or594*	yes	yes
tbb-2	*or600*	yes	yes
zyg-1	*or278, or297, or409, or1018*	yes	yes

[1]Information obtained from: http://www.wormbase.org.
doi:10.1371/journal.pone.0016644.t005

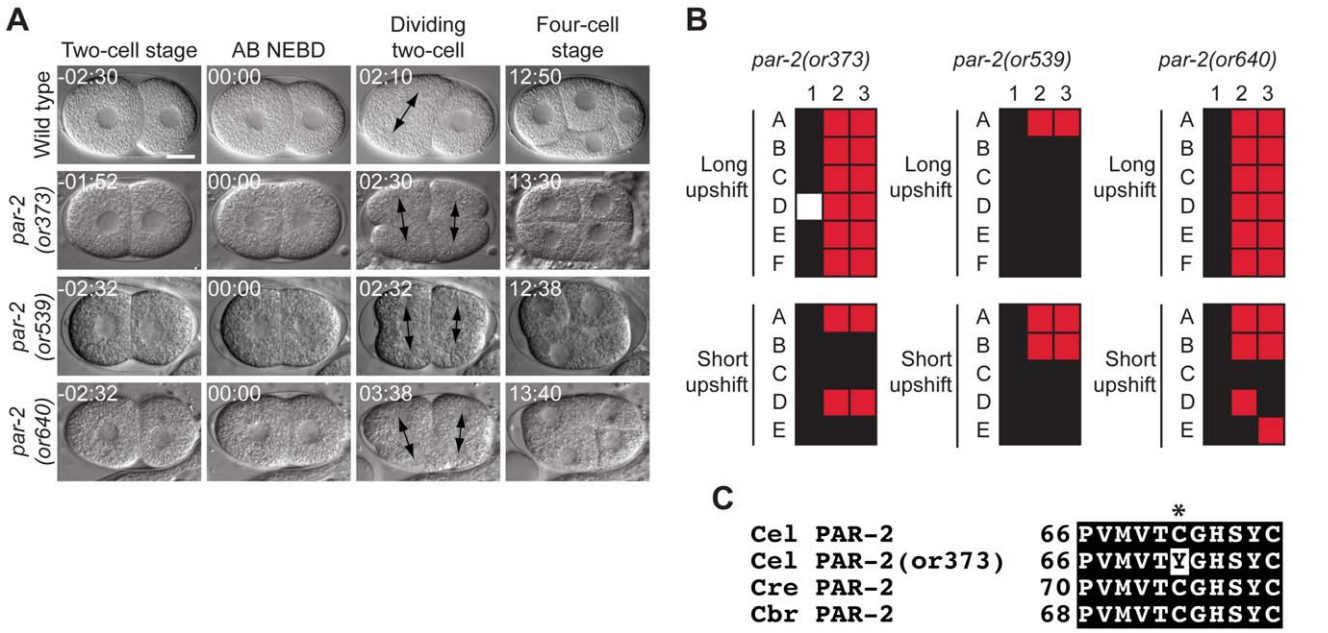

Figure 9. *par-2* mutants. A. DIC time-lapse images of wild-type *par-2(or373* ts*)*, *par-2(or539* ts*)*, and *par-2(or640* ts*)* embryos. The blastomeres in the *par-2* mutants were of similar size at the two cell stage and initiated mitosis simultaneously, in contrast to the wild type. The *par-2(or373* ts*)* embryo was obtained from a hermaphrodite shifted to the restrictive temperature for 5 hours prior to imaging. The *par-2(or539* ts*)* and par-*2(or540* ts*)* embryos were obtained from hermaphrodites shifted to the restrictive temperature for 30 minutes prior to imaging. Arrows indicate mitotic spindles at the two cell stage. Times in min:sec are given relative to AB NEBD. Scale bar, 10 μm. B. Defect map for individual embryos observed during time-lapse recordings, embryos are listed on the left and phenotypes are listed on the top: 1; Normal one cell embryo; 2; assymetric two cell embyro, 3; asynchronous two cell divisions. In the long upshifts, hermaphrodites were transferred to the restrictive temperature for 5–8 hours. In the short upshifts, embryos were harvested from hermaphrodites transferred to the restrictive temperature for 30 minutes. C. Amino acid alteration in the *par-2(or373* ts*)* mutant. Asterisk indicates the changed residue. Homologous proteins are aligned below the *C. elegans* protein.
doi:10.1371/journal.pone.0016644.g009

>10 L4 hermaphrodites to individual plates and grew them at the permissive (15°C) or restrictive (26°C) temperatures until broods were produced. We then removed the worms and allowed the embryos to develop prior to counting viable and inviable progeny. For testing embryonic lethality in heterozygous mothers, we crossed the mutants to a *him-5* strain and tested the F1 progeny as described above. For determining the phenotypes of the TS mutants when shifted to the restrictive temperature from the L1 larval stage, we performed hypochlorite treatments and allowed the embryos to hatch in M9 buffer at 15°C. We then plated~100 synchronized L1 larvae onto a plate and grew them at 26°C until they reached adulthood.

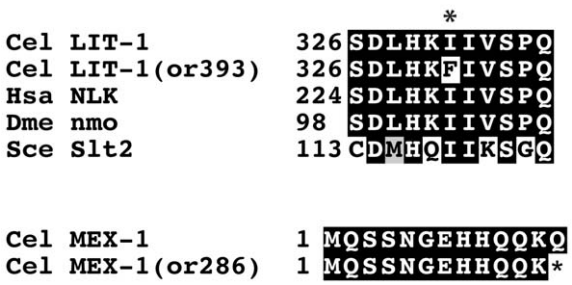

Figure 10. Sequence alterations in the *lit-1(or393* ts*)* and *mex-1(or286* ts*)* mutants. Amino acid alterations in the mutants. Asterisks indicates changed residues. Homologous proteins are aligned below the *C. elegans* protein for LIT-1. A glutamine codon was changed to a stop codon in the *mex-1(or286* ts*)* allele.
doi:10.1371/journal.pone.0016644.g010

Microscopy

Imaging was performed by mounting embryos grown at either 15°C or 26°C on 3% agar pads on microscope slides and sealed with a cover slip. Mounting the embryos was performed at room temperature and usually took 1–2 minutes. Nomarski time lapse images were acquired at a frame rate of 1 image/2 seconds on Zeiss (http://www.zeiss.com) axioskop microscopes equipped with CCD cameras using ImageJ software (http://rsbweb.nih.gov/ij/). Microscopy was performed at room temperature in a room maintained at 24°C. Images were adjusted for contrast in ImageJ.

Mutation identification

Sanger DNA sequencing was performed at the University of Oregon Genomics facility for most genes. We used PCR reactions to amplify 1–2 Kb gene fragments using *Taq* DNA polymerase (Invitrogen). The PCR reactions were run on agarose gels prior to isolating the DNA using a Qiagen QIAquick gel extraction kit. For *plk-1* and *tbb-2*, we used a procedure called interval pull down sequencing which we have developed (manuscript in preparation). Briefly, we isolated mutant genomic DNA, sheared it, annealed it to fosmids containing wild-type genomic DNA and used beads to isolate megabase regions of interest. This purified DNA was subjected to Illumina sequencing at the University of Oregon Genomics facility.

Sequence alignments

We used Wormbase (http://www.wormbase.org/) to obtain homologous proteins encoded in the *Homo sapiens*, *Drosophila melanogaster*, and *Saccharomyces cerevisiae* genomes. In cases where homologous proteins (or homologous domains) were not present,

we performed alignments with other nematode sequences. Protein sequences were aligned with default parameters in CLUSTALW (http://align.genome.jp/) and outputted as alignments using the BOXSHADE package (http://www.ch.embnet.org/software/BOX_form.html).

Acknowledgments

We thank many past members of the Bowerman lab for help in isolating conditional mutants, and current members for useful discussions. We also thank the *Caenorhabditis* Genetics Center at the University of Minnesota, which is funded by the NIH Center for Research Resources and provided many of the strains used for these studies.

Author Contributions

Conceived and designed the experiments: SMO DWT EAJ BB. Performed the experiments: SMO CC LC SNC MPJ BN MHP DWT ARG DRH VRO RL EEM MHN NAS NS JHW JY EAJ BB. Analyzed the data: CC LC BN MHP DWT DRH RL NAS JHW JY EAJ . Wrote the paper: SMO BB.

References

1. Lee T, Winter C, Marticke SS, Lee A, Luo L (2000) Essential roles of *Drosophila* RhoA in the regulation of neuroblast proliferation and dendritic but not axonal morphogenesis. Neuron 25: 307–316.
2. Thomas KR, Capecchi MR (1987) Site-directed mutagenesis by gene targeting in mouse embryo-derived stem cells. Cell 51: 503–512.
3. Eisen JS, Pike SH (1991) The *spt-1* mutation alters segmental arrangement and axonal development of identified neurons in the spinal cord of the embryonic zebrafish. Neuron 6: 767–776.
4. Ho RK, Kane DA (1990) Cell-autonomous action of zebrafish *spt-1* mutation in specific mesodermal precursors. Nature 348: 728–730.
5. Herman RK (1984) Analysis of genetic mosaics of the nematode *Caneorhabditis elegans*. Genetics 108: 165–180.
6. Fire A, Xu S, Montgomery MK, Kostas SA, Driver SE, et al. (1998) Potent and specific genetic interference by double-stranded RNA in *Caenorhabditis elegans*. Nature 391: 806–811.
7. Banaszynski LA, Wandless TJ (2006) Conditional control of protein function. Chem Biol 13: 11–21.
8. Schmidt DJ, Rose DJ, Saxton WM, Strome S (2005) Functional analysis of cytoplasmic dynein heavy chain in *Caenorhabditis elegans* with fast-acting temperature-sensitive mutations. Mol Biol Cell 16: 1200–1212.
9. Severson AF, Hamill DR, Carter JC, Schumacher J, Bowerman B (2000) The aurora-related kinase AIR-2 recruits ZEN-4/CeMKLP1 to the mitotic spindle at metaphase and is required for cytokinesis. Curr Biol 10: 1162–1171.
10. Simon MA, Bowtell DD, Dodson GS, Laverty TR, Rubin GM (1991) Ras1 and a putative guanine nucleotide exchange factor perform crucial steps in signaling by the sevenless protein tyrosine kinase. Cell 67: 701–716.
11. Dorfman M, Gomes JE, O'Rourke S, Bowerman B (2009) Using RNA interference to identify specific modifiers of a temperature-sensitive, embryonic-lethal mutation in the *Caenorhabditis elegans* ubiquitin-like Nedd8 protein modification pathway E1-activating gene *rfl-1*. Genetics 182: 1035–1049.
12. O'Rourke SM, Dorfman MD, Carter JC, Bowerman B (2007) Dynein modifiers in *C. elegans*: light chains suppress conditional heavy chain mutants. PLoS Genet 3: e128.
13. Eki T, Enomoto T, Miyajima A, Miyazawa H, Murakami Y, et al. (1990) Isolation of temperature-sensitive cell cycle mutants from mouse FM3A cells. Characterization of mutants with special reference to DNA replication. J Biol Chem 265: 26–33.
14. Alber T, Sun DP, Nye JA, Muchmore DC, Matthews BW (1987) Temperature-sensitive mutations of bacteriophage T4 lysozyme occur at sites with low mobility and low solvent accessibility in the folded protein. Biochemistry 26: 3754–3758.
15. Bonatti S, Simili M, Abbondandolo A (1972) Isolation of temperature-sensitive mutants of *Schizosaccharomyces pombe*. J Bacteriol 109: 484–491.
16. Hartwell LH (1967) Macromolecule synthesis in temperature-sensitive mutants of yeast. J Bacteriol 93: 1662–1670.
17. Nasmyth K, Nurse P (1981) Cell division cycle mutants altered in DNA replication and mitosis in the fission yeast *Schizosaccharomyces pombe*. Mol Gen Genet 182: 119–124.
18. Hartwell LH, Mortimer RK, Culotti J, Culotti M (1973) Genetic Control of the Cell Division Cycle in Yeast: V. Genetic Analysis of *cdc* Mutants. Genetics 74: 267–286.
19. Hartwell LH, Culotti J, Reid B (1970) Genetic control of the cell-division cycle in yeast. I. Detection of mutants. Proc Natl Acad Sci U S A 66: 352–359.
20. Hillman R (1962) A genetically controlled head abnormality in Drosophila melanogaster. II. Temperature sensitive periods during the development of notch-deformed. Genetics 47: 11–23.
21. Mains PE, Sulston IA, Wood WB (1990) Dominant maternal-effect mutations causing embryonic lethality in *Caenorhabditis elegans*. Genetics 125: 351–369.
22. Cassada R, Isnenghi E, Culotti M, von Ehrenstein G (1981) Genetic analysis of temperature-sensitive embryogenesis mutants in *Caenorhabditis elegans*. Dev Biol 84: 193–205.
23. Isnenghi E, Cassada R, Smith K, Denich K, Radnia K, et al. (1983) Maternal effects and temperature-sensitive period of mutations affecting embryogenesis in *Caenorhabditis elegans*. Dev Biol 98: 465–480.
24. Kemphues KJ, Priess JR, Morton DG, Cheng NS (1988) Identification of genes required for cytoplasmic localization in early *C. elegans* embryos. Cell 52: 311–320.
25. Encalada SE, Martin PR, Phillips JB, Lyczak R, Hamill DR, et al. (2000) DNA replication defects delay cell division and disrupt cell polarity in early *Caenorhabditis elegans* embryos. Dev Biol 228: 225–238.
26. Shirayama M, Soto MC, Ishidate T, Kim S, Nakamura K, et al. (2006) The Conserved Kinases CDK-1, GSK-3, KIN-19, and MBK-2 Promote OMA-1 Destruction to Regulate the Oocyte-to-Embryo Transition in *C. elegans*. Curr Biol 16: 47–55.
27. Golden A, Sadler PL, Wallenfang MR, Schumacher JM, Hamill DR, et al. (2000) Metaphase to anaphase (mat) transition-defective mutants in *Caenorhabditis elegans*. J Cell Biol 151: 1469–1482.
28. Timmons L, Fire A (1998) Specific interference by ingested dsRNA. Nature 395: 854.
29. Kamath RS, Fraser AG, Dong Y, Poulin G, Durbin R, et al. (2003) Systematic functional analysis of the *Caenorhabditis elegans* genome using RNAi. Nature 421: 231–237.
30. Maeda I, Kohara Y, Yamamoto M, Sugimoto A (2001) Large-scale analysis of gene function in *Caenorhabditis elegans* by high-throughput RNAi. Curr Biol 11: 171–176.
31. Gönczy P, Echeverri G, Oegema K, Coulson A, Jones SJ, et al. (2000) Functional genomic analysis of cell division in *C. elegans* using RNAi of genes on chromosome III. Nature 408: 331–336.
32. Sonnichsen B, Koski LB, Walsh A, Marschall P, Neumann B, et al. (2005) Full-genome RNAi profiling of early embryogenesis in *Caenorhabditis elegans*. Nature 434: 462–469.
33. Sarin S, Prabhu S, O'Meara MM, Pe'er I, Hobert O (2008) *Caenorhabditis elegans* mutant allele identification by whole-genome sequencing. Nat Methods 5: 865–867.
34. Ellis GC, Phillips JB, O'Rourke S, Lyczak R, Bowerman B (2004) Maternally expressed and partially redundant β-tubulins in *Caenorhabditis elegans* are autoregulated. J Cell Sci 117: 457–464.
35. Phillips JB, Lyczak R, Ellis GC, Bowerman B (2004) Roles for two partially redundant alpha-tubulins during mitosis in early *Caenorhabditis elegans* embryos. Cell Motil Cytoskeleton 58: 112–126.
36. Kao G, Tuck S, Baillie D, Sundaram MV (2004) *C. elegans* SUR-6/PR55 cooperates with LET-92/protein phosphatase 2A and promotes Raf activity independently of inhibitory Akt phosphorylation sites. Development 131: 755–765.
37. Sieburth DS, Sundaram M, Howard RM, Han M (1999) A PP2A regulatory subunit positively regulates Ras-mediated signaling during *Caenorhabditis elegans* vulval induction. Genes Dev 13: 2562–2569.
38. Schlaitz AL, Srayko M, Dammermann A, Quintin S, Wielsch N, et al. (2007) The *C. elegans* RSA complex localizes protein phosphatase 2A to centrosomes and regulates mitotic spindle assembly. Cell 128: 115–127.
39. Schroer TA (2004) Dynactin. Annu Rev Cell Dev Biol 20: 759–779.
40. Skop AR, White JG (1998) The dynactin complex is required for cleavage plane specification in early *Caenorhabditis elegans* embryos. Curr Biol 8: 1110–1116.
41. Encalada SE, Willis J, Lyczak R, Bowerman B (2005) A spindle checkpoint functions during mitosis in the early *Caenorhabditis elegans* embryo. Mol Biol Cell 16: 1056–1070.
42. Koushika SP, Schaefer AM, Vincent R, Willis JH, Bowerman B, et al. (2004) Mutations in *Caenorhabditis elegans* cytoplasmic dynein components reveal specificity of neuronal retrograde cargo. J Neurosci 24: 3907–3916.
43. McNally K, Audhya A, Oegema K, McNally FJ (2006) Katanin controls mitotic and meiotic spindle length. J Cell Biol 175: 881–891.
44. Quintin S, Mains PE, Zinke A, Hyman AA (2003) The *mbk-2* kinase is required for inactivation of MEI-1/katanin in the one-cell *Caenorhabditis elegans* embryo. EMBO Rep 4: 1175–1181.
45. Srayko M, Buster DW, Bazirgan OA, McNally FJ, Mains PE (2000) MEI-1/MEI-2 katanin-like microtubule severing activity is required for *Caenorhabditis elegans* meiosis. Genes Dev 14: 1072–1084.
46. McNally FJ, Vale RD (1993) Identification of katanin, an ATPase that severs and disassembles stable microtubules. Cell 75: 419–429.
47. Mains PE, Kemphues KJ, Sprunger SA, Sulston IA, Wood WB (1990) Mutations affecting the meiotic and mitotic divisions of the early *Caenorhabditis elegans* embryo. Genetics 126: 593–605.
48. Bettencourt-Dias M, Glover DM (2007) Centrosome biogenesis and function: centrosomics brings new understanding. Nat Rev Mol Cell Biol 8: 451–463.

49. Kemp CA, Kopish KR, Zipperlen P, Ahringer J, O'Connell KF (2004) Centrosome maturation and duplication in *C. elegans* require the coiled-coil protein SPD-2. Dev Cell 6: 511–523.
50. O'Connell KF, Maxwell KN, White JG (2000) The *spd-2* gene is required for polarization of the anteroposterior axis and formation of the sperm asters in the *Caenorhabditis elegans* zygote. Dev Biol 222: 55–70.
51. Pelletier L, Ozlu N, Hannak E, Cowan C, Habermann B, et al. (2004) The *Caenorhabditis elegans* centrosomal protein SPD-2 is required for both pericentriolar material recruitment and centriole duplication. Curr Biol 14: 863–873.
52. Bettencourt-Dias M, Rodrigues-Martins A, Carpenter L, Riparbelli M, Lehmann L, et al. (2005) SAK/PLK4 is required for centriole duplication and flagella development. Curr Biol 15: 2199–2207.
53. O'Connell KF, Caron C, Kopish KR, Hurd DD, Kemphues KJ, et al. (2001) The *C. elegans zyg-1* gene encodes a regulator of centrosome duplication with distinct maternal and paternal roles in the embryo. Cell 105: 547–558.
54. Chase D, Serafinas C, Ashcroft N, Kosinski M, Longo D, et al. (2000) The polo-like kinase PLK-1 is required for nuclear envelope breakdown and the completion of meiosis in *Caenorhabditis elegans*. Genesis 26: 26–41.
55. Budirahardja Y, Gonczy P (2008) PLK-1 asymmetry contributes to asynchronous cell division of *C. elegans* embryos. Development 135: 1303–1313.
56. Nishi Y, Rogers E, Robertson SM, Lin R (2008) Polo kinases regulate *C. elegans* embryonic polarity via binding to DYRK2-primed MEX-5 and MEX-6. Development 135: 687–697.
57. Rivers DM, Moreno S, Abraham M, Ahringer J (2008) PAR proteins direct asymmetry of the cell cycle regulators Polo-like kinase and Cdc25. J Cell Biol 180: 877–885.
58. Kemphues KJ, Priess JR, Morton DG, Cheng NS (1988) Identification of genes required for cytoplasmic localization in early *C. elegans* embryos. Cell 52: 311–320.
59. Levitan DJ, Boyd L, Mello CC, Kemphues KJ, Stinchcomb DT (1994) *par-2*, a gene required for blastomere asymmetry in *Caenorhabditis elegans*, encodes zinc-finger and ATP-binding motifs. Proc Natl Acad Sci U S A 91: 6108–6112.
60. Boyd L, Guo S, Levitan D, Stinchcomb DT, Kemphues KJ (1996) PAR-2 is asymmetrically distributed and promotes association of P granules and PAR-1 with the cortex in *C. elegans* embryos. Development 122: 3075–3084.
61. Kaletta T, Schnabel H, Schnabel R (1997) Binary specification of the embryonic lineage in *Caenorhabditis elegans*. Nature 390: 294–2948.
62. Meneghini MD, Ishitani T, Carter JC, Hisamoto N, Ninomiya-Tsuji J, et al. (1999) MAP kinase and Wnt pathways converge to downregulate an HMG-domain repressor in *Caenorhabditis elegans*. Nature 399: 793–797.
63. Rocheleau CE, Yasuda J, Shin TH, Lin R, Sawa H, et al. (1999) WRM-1 activates the LIT-1 protein kinase to transduce anterior/posterior polarity signals in *C. elegans*. Cell 97: 717–726.
64. Guedes S, Priess JR (1997) The *C. elegans* MEX-1 protein is present in germline blastomeres and is a P granule component. Development 124: 731–739.
65. Mello CC, Draper BW, Krause M, Weintraub H, Priess JR (1992) The *pie-1* and *mex-1* genes and maternal control of blastomere identity in early *C. elegans* embryos. Cell 70: 163–176.
66. Schnabel R, Weigner C, Hutter H, Feichtinger R, Schnabel H (1996) *mex-1* and the general partitioning of cell fate in the early *C. elegans* embryo. Mech Dev 54: 133–147.
67. Brenner S (1974) The genetics of *Caenorhabditis elegans*. Genetics 77: 71–94.